COMPRESSIVE SENSING-BASED IMAGE DENOISING USING ADAPTIVE MULTIPLE SAMPLING AND OPTIMAL ERROR TOLERANCE

Wonseok Kang⋆*, Eunsung Lee*⋆*, Eunjung Chea*⋆*, Aggelos K. Katsaggelos*†*, and Joonki Paik*⋆

⋆ Image Processing and Intelligent Systems Laboratory, Graduate School of Advanced Imaging Science, Multimedia, and Film Seoul, Chung-Ang University, Korea

† Department of Electrical Engineering and Computer Science, Northwestern University, Evanston, IL 60208, USA

ipis.kang@gmail.com⋆, lessel7@gmail.com⋆, cej8838@gmail.com⋆, aggk@eece.northwestern.edu†, and paikj@cau.ac.kr⋆

ABSTRACT

In this paper, we present a compressive sensing-based image denoising algorithm using spatially adaptive image representation and estimation of optimal error tolerance based on sparse signal analysis. The proposed method performs block-based multiple compressive sampling after decomposing the sparse signal into feature and non-feature regions using simple statistical analysis. For minimization of recovery error and number of iterations, the modified OMP method estimates the optimal error tolerance using the average variance in the recovery step. Experimental results demonstrate that the proposed denoising algorithm better removes noise without undesired artifacts than existing state-of-the-art methods in terms of both objective (PSNR/SSIM) and subjective measures. Processing time of the proposed method is 5 to 10 times faster than the standard OMP-based method.

***Index Terms*—** Compressed sensing, matching pursuit algorithms, image denoising

1. INTRODUCTION

Based on the theory of compressive sensing (CS) a sparse signal can be reconstructed from far fewer samples than the samples required by the Nyquist rate [1] [2]. For this reason CS theory has been widely applied to computational photography [3], medical imaging [4] and remote sensing [5], to name a few. In a CS-based image processing system, denoising is very important to improve the quality of images using a reduced amount of data. Especially, it is a challenging problem to remove the noise while preserving image details because of the high-frequency characteristics of the noise.

In this paper, we present a CS-based image denoising algorithm using spatially adaptive image reconstruction and optimal error tolerance in the sense of sparse signal representation. For preserving image features, the proposed method decomposes the sparse signal into feature and non-feature regions using statistical analysis and sparse representation. The proposed method computes the measurement signals from the decomposed sparse signals using block-based multiple compressive samplings. The original noise-free image is recovered using orthogonal matching pursuit (OMP) [6] with optimal error tolerance.

Experimental results show that the proposed CS-based image denoising algorithm can better remove noise while preserving perceptual quality than existing state-of-the-art methods. The proposed method consists of two steps: (i) the block based multiple compressive sampling step after decomposing a sparse signal into feature and non-feature regions and (ii) the recovery step of the original sparse signal using OMP with optimally estimated error tolerance. The proposed CS-based image denoising algorithm is shown in Fig. 1.

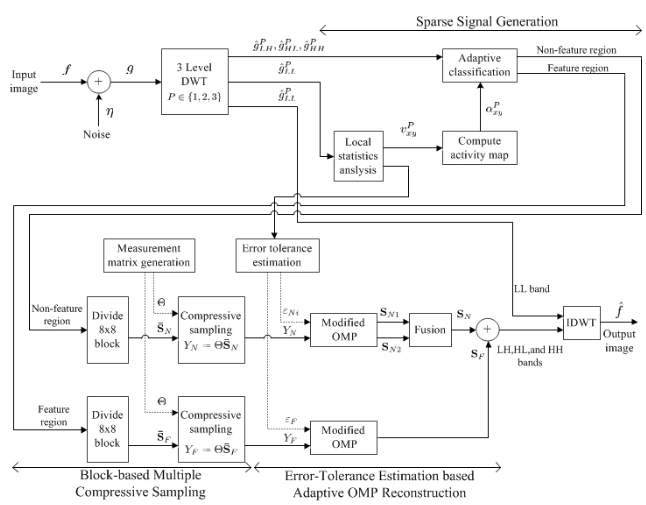

Fig. 1. Block diagram of the proposed CS-based image denoising algorithm.

2. DECOMPOSITION OF A SPARSE SIGNAL AND MULTIPLE COMPRESSIVE SAMPLING

Let f be the original image, η the noise, and g the observed image with additive noise, then the image degradation model is expressed as

$$g = f + \eta. \tag{1}$$

In general, the noisy image g is transformed into a k-sparse signal with only k non-zero values using an orthogonal transformation such as the discrete Fourier transform (DFT), discrete cosine transform (DCT), and discrete wavelet transform (DWT) [1] [2].

In this paper, we use a three-level DWT to decompose the sparse signal into feature and non-feature regions. For considering both, implementational efficiency and acceptable degree of sparsity, we can generate a two-dimensional (2D) scaling function and three directional wavelet functions using one-dimension (1D) 8-tap symmetrical wavelet (symlet) filters [9]. Three levels of the DWT coefficients are respectively expressed as

$$\hat{g}^1 = W^1 g = [\hat{g}^1_{LL}\ \hat{g}^1_{LH}\ \hat{g}^1_{HL}\ \hat{g}^1_{HH}]^T, \tag{2}$$

$$\hat{g}^2 = W^2 \hat{g}^1_{LL} = [\hat{g}^2_{LL}\ \hat{g}^2_{LH}\ \hat{g}^2_{HL}\ \hat{g}^2_{HH}]^T, \tag{3}$$

and

$$\hat{g}^3 = W^3 \hat{g}^2_{LL} = [\hat{g}^3_{LL}\ \hat{g}^3_{LH}\ \hat{g}^3_{HL}\ \hat{g}^3_{HH}]^T, \tag{4}$$

where W^P, $P \in \{1,2,3\}$, represents the 2D DWT matrix of level P. For decomposing the sparse signal and block-based multiple compressive sampling, we compute the variance of a local rectangular $p \times q$ block in $\hat{g}^P_{LL}$ to decompose the sparse signal into feature and non-feature regions as

$$v^P_{xy} = \frac{1}{pq} \sum_{(i,j)\in R_{xy}} \left\{\hat{g}^P_{LL}(i,j) - m_{xy}\right\}^2, \tag{5}$$

where R_{xy} represents an $p \times q$ rectangular region centered at (x, y), and m_{xy} is the local mean. We compute the activity map of $\hat{g}^P_{LL}$ using the local variance value as

$$\alpha^P_{xy} = \frac{1}{1 + \theta v^P_{xy}}, \tag{6}$$

where the tuning parameter θ is chosen so that the activity value is distributed uniformly in [0,1], and v^P_{xy} is the variance value. Equation (6) was also used in [10] in the context of adaptive image restoration. The sparse signals of the LH, HL and HH sub-bands in each DWT level P are decomposed into feature and non-feature regions based on the activity map.

The decomposed sparse signals are divided into blocks of 8×8 pixels for block-based multiple compressive sampling. The Block-based CS method [11] [12] can significantly reduce the processing time at the cost of segmentation accuracy. Since only one $\hat{g}^3_{LL}$ does not satisfy the sparsity condition and takes only 1.5% of the total region, we perform multiple compressive sampling to obtain the sparse signal of compression ratio $r/64$ to only the LH, HL, and HH sub-bands using a Gaussian measurement matrix as follows

$$Y_{D,B} = \Theta \bar{\mathbf{S}}_{D,B}, \text{for } D \in \{F, N\}, B \in \{1, 2, ..., K\}, \tag{7}$$

where Θ represents the $r \times 64$ Gaussian measurement matrix, $D \in \{F, N\}$ one of the feature (F) and non-feature (N) region, B the number of divided blocks, $\bar{\mathbf{S}}_{D,B}$ the 64×1 1D vector for the corresponding 8×8 block of LH, HL, and HH sub-bands and $Y_{D,B}$ the $r \times 1$ sampled measurement signals with compression ratio of $r/64$. For the block-based multiple compressive sampling, we used the measurement matrix of Gaussian probability distribution [6]. These measurement matrices satisfy the restricted isometry property (RIP) condition [13], and the original sparse signals can be successfully recovered form measurement signals.

3. MODIFIED OMP BY ESTIMATING THE OPTIMAL ERROR TOLERANCE

Recovery of the sparse signals $\mathbf{S}_{D,B}$ from (7) is an ill-posed problem. But the recovery of $\mathbf{S}_{D,B}$ is possible by minimizing the l_0-norm of the residual, since $\mathbf{S}_{D,B}$ is sparse. The l_0 minimization method is, however, an NP-Hard (non-deterministic polynomial-time hard) problem, and the l_1 minimization method is used as

$$\mathbf{S}_{D,B} = \arg\min \left\|\bar{\mathbf{S}}_{D,B}\right\|_1 \ s.t.\ \left\|Y_{D,B} - \Theta\bar{\mathbf{S}}_{D,B}\right\|_2 \le \varepsilon. \tag{8}$$

For deducing the computational complexity, a fast block-based OMP recovery method has been proposed in [11] [12]. However it cannot successfully recover the original sparse signal with a certain amount of noise since the recovery error becomes larger than the error tolerance. In this paper, we present a modified OMP method by estimating the optimal error tolerance using a property of sparse signal and the amount of noise.

As shown in Table 1, the modified OMP reconstruction method consists of four steps. In the initialization step, the index set I is set to be the empty set, and the measurement signal $Y_{D,B}$ is assigned to the residual vector $\mathbf{r}$. Step 1 estimates the optimal error tolerance that will be used for the termination condition in both feature and non-feature regions. Since compressively sampled block measurement signals are 8×8 block sparse signals from $\hat{g}^P_{LH}, \hat{g}^P_{HL}$ and $\hat{g}^P_{HH}$ before compressive sampling, we can estimate the statistical characteristics of measured block $Y_{D,B}$ using variance of the corresponding $\hat{g}^P_{LL}$.

The sampled measurement signals $Y_{F,B}$ of feature regions can be classified into one of edge, details, and noise components based on the property of the activity map generated from the local variance value [10]. For reconstructing a sparse signal from measurement signals $Y_{F,B}$ with preserving the

Table 1. Modified OMP Method

Input : Θ : measurement matrix
$Y_{D,B}$: measurement signal vector
ε : error tolerance
Output : $\mathbf{S}_{D,B}$: solution vector
Initialization : index data set $I = \varnothing$, residual $\mathbf{r} = Y_{D,B}$, and error tolerance $\varepsilon = 0.1$
repeat $D = F, N$ repeat $B = 1, 2, ..., K$
step 1 : estimating the optimal error tolerance
error tolerance of feature region
$\varepsilon_F \leftarrow \frac{1}{E[v_{xy}^P]} \times \varepsilon$
error tolerance of non-feature region
$(\varepsilon_{N1},\ \varepsilon_{N2}) \leftarrow (E[v_{xy}^P] \times \varepsilon) w_i$
step 2 : main interaction
$\lambda \leftarrow$ largest coordinate $\lvert\Theta^* \mathbf{r}\rvert$
$I \leftarrow I\ \cup\ \lambda$
$\mathbf{S}_{D,B} = \arg\min \left\lVert Y_{D,B} - \Theta\rvert_I \bar{\mathbf{S}}_{D,B} \right\rVert_2$
step 3 : residual update and check the stop rule
$\mathbf{r} = Y_{D,B} - \Theta \bar{\mathbf{S}}_{D,B}$
if $Y_{D,B}, D == F$
$\lVert\mathbf{r}\rVert^2 \leq \varepsilon_F \rightarrow \mathbf{S}_{F,B}$ end algorithm
if $Y_{D,B}, D == N$
$\lVert\mathbf{r}\rVert^2 \leq \varepsilon_{N1} \rightarrow \mathbf{S}_{N1,B}$
repeat
$\lVert\mathbf{r}\rVert^2 \leq \varepsilon_{N2} \rightarrow \mathbf{S}_{N2,B}$ go step 4
step 4 : minimization recovery error
$\mathbf{S}_{N,B} = \frac{1}{2} \sum \left[\mathbf{S}_{N1,B} + \mathbf{S}_{N2,B}\right]$ end algorithm

feature components, the error tolerance value should become as small as possible for minimizing the reconstruction residual $\mathbf{r}$ in the OMP recovery process. For the estimation of the optimal error tolerance of the $B, B \in \{1, 2, ..., K\}$-th block in the feature region of $\hat{g}_{LH}^P, \hat{g}_{HL}^P$ and $\hat{g}_{HH}^P$, we compute the mean of variances of K blocks located at the corresponding $\hat{g}_{LL}^P$. We then estimate the optimal error tolerance that will be used to recover the measured signal from the B-th block using the reciprocal value of the computed mean of variance as

$$\varepsilon_F = \frac{1}{E[v_{xy}^P]} \times \varepsilon, \tag{9}$$

where $E[v_{xy}^p]$ represents the average variance of a block in $\hat{g}_{LL}^P$ whose location is determined by the B-th block in $\hat{g}_{LH}^P, \hat{g}_{HL}^P$ and $\hat{g}_{HH}^P$, and ε the constant for adjusting the initial error tolerance. In this paper, we used $\epsilon = 0.1$ for the experiments. On the other hand the sampled measurement signals $Y_{N,B}$ in the non-feature region includes a lot of noise components based on the property of the activity map. If we use the error tolerance given in (9), it is impossible to correctly recover the original sparse signal, and the termination condition is not suitable for the OMP algorithm because of the high reconstruction residual vector $\lVert\mathbf{r}\rVert^2$ caused by the noise energy. For removing the noise effect in the OMP recovery process, the error tolerance value should satisfy $\varepsilon_N \geq \lVert\eta\rVert^2$ by using the average variance $E[v_{xy}^p]$ containing noise energy. In the OMP process for non-feature region, we estimate two error tolerance values using simple weighting as

$$\varepsilon_{Ni} = (E[v_{xy}^P] \times \varepsilon) w_i, \text{ for } i \in \{1, 2\}, \tag{10}$$

where w_i represents the weight value. We used $w_1 = 0.8$ and $w_2 = 1.5$ for the experiment. For removing artifacts caused by reconstruction error, we combine two differently recovered sparse signals from a sampled measurement $Y_{N,B}$ in the non-feature region in step 4. In step 2, the modified OMP computes the largest coordinate of $\lvert\Theta^* \mathbf{r}\rvert$ and the location of the largest value is added in the index set I. In step 3 the modified OMP computes a new provisional solution $\mathbf{S}_{D,B}$ by minimizing $\left\lVert Y_{D,B} - \Theta\rvert_I \bar{\mathbf{S}}_{D,B} \right\rVert_2$, and updates the residual vector $\mathbf{r} = Y_{D,B} - \Theta \bar{\mathbf{S}}_{D,B}$. For recovering the sparse signal $\mathbf{S}_{F,B}$ in the feature region from an input measurement signal $Y_{F,B}$, the updated residual vector is computed as

$$\mathbf{r}^t = Y_{F,B} - \Theta \bar{\mathbf{S}}_{F,B}^t, \tag{11}$$

where $\mathbf{r}^t$ represents the updated residual vector at the t-th iteration, $Y_{F,B}$ a sampled measurement signal in the feature region, and Θ the measurement matrix. Based on (11) the following termination condition is checked in each iteration

$$\left\lVert \mathbf{r}^t \right\rVert^2 < \epsilon_F, \tag{12}$$

where $\lVert\mathbf{r}^t\rVert^2$ represents the l_2-norm of the updated residual, and ϵ_F the estimated error tolerance that can be adaptively changed by the variance for minimizing the residual $\mathbf{r}^t$. As a result, the recovered sparse signals preserve feature components of measurement signals $Y_{F,B}$ by using the optimal error tolerance. In the recovery of measurement signals in the non-feature region, the modified OMP repeats steps 2 and 3 using the estimated error tolerance ε_{N1} and ε_{N2}, $(\varepsilon_{N1} < \varepsilon_{N2})$. In step 3, that is the updating stage, we can obtain two differently recovered sparse signals from one sampled measurement signal of non-feature region $Y_{N,B}$ using the relationship of weighted error tolerance values. In step 4, the two recovered sparse signals are fused for minimizing the artifacts as

$$\mathbf{S}_{N,B} = \frac{1}{2} \sum \left[\mathbf{S}_{N1,B} + \mathbf{S}_{N2,B}\right], \tag{13}$$

where $\mathbf{S}_{N1,B}$ and $\mathbf{S}_{N2,B}$ represent recovered sparse signals from measurement signals in the non-feature region $Y_{N,B}$ using error tolerances ε_{N1} and ε_{N2}, respectively. The recovered sparse signals of each region are combined to generate the DWT sub-bands, and the final noise-free image is obtained using the inverse discrete wavelet transform (IDWT).

4. EXPERIMENTAL RESULT

For evaluating performance of the proposed method, we used the 512x512 Lena image and compression ratio $r/64$=0.5

with various amounts of noise. In the experiment we evaluated the performances of the standard OMP [6] and the proposed methods in the sense of computation time, peak signal-to-noise ratio (PSNR), and mean structural similarity index (SSIM) [14]. For decomposing sparse signals, we used the activity map tunning parameter of $\theta = \{500, 300, 150\}$ in each DWT level, $P \in \{1, 2, 3\}$. For the initializing of error tolerance, $\varepsilon = 0.1$ was used.

(a) (b) (c) (d)

Fig. 2. Experimental results: (a) original image, (b) simulated degraded image with AWGN (15dB), (c) reconstructed image using the OMP method, and (d) reconstructed image using the proposed method.

As shown in Fig. 2, the proposed method produces an almost noise-free result while preserving sharp edges whereas the original OMP method cannot perfectly remove noise while producing blurry edges. Processing time of the proposed method is approximately 10 times faster than original OMP-based method with 15dB additive white Gaussian noise (AWGN) noise. Table 2 summarizes the PSNR/SSIM values and the computational times of the original OMP and the proposed methods.

Table 2. Comparison of the standard OMP and the proposed methods in sense of PSNR, MSSIM and processing time(Sec)

Noise(dB)	Method	PSNR	SSIM	Time
15	OMP	25.7600	0.7863	61.32
	Proposed	30.3172	0.9368	6.50
20	OMP	28.2546	0.8632	61.76
	Proposed	31.5899	0.9524	8.41
25	OMP	29.4149	0.8879	61.58
	Proposed	32.3330	0.9671	11.08
30	OMP	30.1056	0.9002	63.32
	Proposed	32.3544	0.9714	11.56

Fig. 3 shows additional experimental results which compare the proposed method with the state-of-the art denoising methods including SADCT [7] and BM3D [8]. As shown in the experimental result, the proposed method provides better noise removal performance than existing state-of-the-art methods. In the eye region of the Mandril, conventional denoising methods cannot preserve the feature components whereas the proposed method can both remove noise and preserve features. Table 3 summarizes the PSNR/SSIM values for the SADCT, BM3D and the proposed methods.

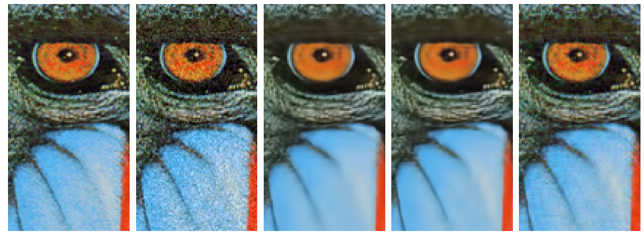

(a) (b) (c) (d) (e)

Fig. 3. Experimental results: (a) original image, (b) simulated degraded image with AWGN (15dB), (c) result of the SADCT [7], (d) result of the BM3D [8] and (e) result of the proposed method.

Table 3. The PSNR / SSIM values comparison of two different method

Noise(dB)	Method	PSNR	SSIM
	SADCT	25.0100	0.7577
15	BM3D	25.1113	0.7607
	Proposed	26.7019	0.8390

5. CONCLUSION

In this paper, we presented a compressive sensing-based image denoising algorithm using spatially adaptive image representation and estimation of optimal error tolerance based on sparse signal analysis. The proposed method performs a block-based multiple compressive sampling after decomposing the sparse signal into feature and non-feature regions using the activity map. As a result, the proposed method can reconstruct the noise-free sparse signal by estimating the optimal error tolerance in the OMP step for minimizing both recovery error and the number of iterations. Experimental results demonstrate that the proposed method can better remove noise than existing state-of-the-art methods in terms of both PSNR and SSIM. Processing time of the proposed method is 5 to 10 times faster than original OMP-based method and is suitable for various CS-based image system such as medical imaging, remote sensing, and image enhancement and restoration.

6. ACKNOWLEDGE

This research was supported by Basic Science Research Program through National Research Foundation (NRF) of Korea funded by the Ministry of Education, Science and Technology (2009-0081059) and by Korea Aerospace Research Institute in the Korea Multi-Purpose Satellite-3A(KOMPSAT-3A) project.

7. REFERENCES

[1] E. Candes and T. Tao, ”Decoding by linear programming,” *IEEE Trans. Information Theory*, vol. 51, no. 12, pp. 4203-4215, December 2005.

[2] E. Candes and M. Wakin, ”An introduction to compressive sampling,” *IEEE Signal Processing Magazine*, vol. 25, no. 2, pp. 21-30, March 2008.

[3] M. Duarte, M. Davenport, D. Takhar, J. Laska, T. Sun, K. Kelly, and R. Baraniuk, Single-pixel imaging via compressive sampling, *IEEE Signal Processing Magazine*, vol. 25, no. 2, pp. 8391, 2008.

[4] M. Lustig, D. Donoho, and J. Pauly, Sparse MRI: The application of compressed sensing for rapid MR imaging, *Magnetic Resonance in Medicine*, vol. 58, no. 6, pp. 11821195, December 2007.

[5] M. T. Alonso, P. L. Dekker and J. J. Mallorqui, ” A Novel Strategy for Radar Imaging Based on Compressive Sensing, *IEEE Trans. Geoscience and Remote Sensing*, vol. 48, no. 12, pp. 4285-4295, December 2010.

[6] J. Tropp and A. Gilbert, ”Signal recovery form random measurements via orthogonal matching pursuit,” *IEEE Trans. Information Theory*, vol. 53, no. 12, pp. 4655-4666, December 2007.

[7] A. Foi, V. Katkovnik, and K. Egiazarian, ”Pointwise Shape-Adaptive DCT for High-Quality Denoising and Deblocking of Grayscale and Color Images,” *IEEE Trans. Image Processing*, vol. 16, no. 5, pp. 1395-1411, May 2007.

[8] K. Dabov, A. Foi, V. Katkovnik, and K. Egiazarian, ”Image Denoising by Sparse 3-D Transform-Domain Collaborative Filtering” *IEEE Trans. Image Processing*, vol. 16, no. 8, pp. 2080-2095, August 2007.

[9] S. Mallat, A Wavelet Tour of Signal Processing, *New York: Academic Press*, 1998.

[10] S. N. Efstratiadis and A. K. Katsaggelos, ”Adaptive iterative image restoration with reduced computational load,” *Optical engineering*, vol. 29, no. 12, pp. 1458-1468, December 1990.

[11] L. Gan, T. Do, and T. Tran, ”Fast compressive image using scrambled block Hadamard ensemble,” *in Proc. EUSIPCO*, 2008.

[12] S. Mun and J. Fowler, ”Block compressed sensing of images using directional transforms,” *in Proc. ICIP*, pp. 3021-3024, 2009.

[13] E. Candes, J. Romberg, and T. Tao, ”Robust uncertainty principles: Exact signal reconstruction from highly incomplete frequency information,” *IEEE Trans. Information Theory*, vol. 52, no. 2, pp. 489-509, February 2006.

[14] Z. Wang, A. Bovik, H. Sheikh, and E. Simoncelli, ”Image quality assessment: from error visibility to structural similarity,” *IEEE Trans. Image Processing*, vol. 13, no. 4, pp. 600-612, April 2004.